基于 GS-SVM 的脑组织差分路径因子定量方法研究

储宝[1,2]，黄尧[2,3*]，倪敬书[2,3]，张持健[1]，李忠胜[2,3]，张元志[2,3]，
董美丽[2,3]，王全福[2,3]，王霞[2,3]，王贻坤[2,3**]

[1]安徽师范大学物理与电子信息学院，安徽 芜湖 241000；
[2]中国科学院合肥物质科学研究院安徽光学精密机械研究所安徽省医用光学诊疗技术与装备工程实验室，安徽 合肥 230026；
[3]皖江新兴产业技术发展中心安徽省生物医学光学仪器工程技术研究中心，安徽 铜陵 244000

摘要 差分路径因子（Differential Pathlength Factor，DPF）是用于计算脑血氧生理参数的重要变量之一，可通过蒙特卡罗模拟计算得到，但此方法存在耗时长、提取参数复杂等缺点。针对以上不足，提出了一种 DPF 快速定量计算方法。首先对不同年龄段人群的脑组织光学参数与颅骨厚度进行归一化处理与主成分分析，采用支持向量机（Support Vector Machine，SVM）并结合网格寻优（Grid Search，GS），建立了基于 GS-SVM 的脑组织差分路径因子的预测模型，对测试样本数据进行了回归预测，最后将所得结果与反向传播人工神经网络（Back Propagation Artificial Neural Network，BP-ANN）的预测结果进行了对比。结果表明，相较于蒙特卡罗模拟，GS-SVM 预测模型与 BP-ANN 预测模型的均方误差（MSE）分别为 0.0268 与 0.25，相关系数（R^2）分别为 0.97 与 0.92。基于 GS-SVM 的脑组织差分路径因子定量模型的预测结果优于 BP-ANN，与蒙特卡罗模拟结果呈显著性相关（显著水平 $P < 0.0001$），有望取代传统蒙特卡罗模拟对 DPF 进行快速批量预测。

关键词 医用光学；近红外光谱；差分路径因子；蒙特卡罗模拟；支持向量机；网格寻优

中图分类号 TN29　　　**文献标志码** A　　　　　　　　　　**doi**：10.3788/CJL202249.0507008

1 引　　言

　　脑的耗氧量约占人体总耗氧量的四分之一，大脑对缺氧高度敏感，短时间内的缺氧就可造成不可逆的神经损伤[1-3]。基于近红外光谱（Near Infrared Spectroscopy，NIRS）技术的脑血氧监测可无创、连续、实时地显示脑内氧供需状态，对术中的脑保护至关重要，具有极高的应用价值[4]。在组织光学中，780～1000 nm 的近红外光对人体组织具有良好的穿透性，且在该波段下，生物组织内的主要吸收物质是还原血红蛋白与氧合血红蛋白[5]。因此，利用还原血红蛋白与氧合血红蛋白吸收的差异，结合修正比尔朗伯（Modified Beer-Lambert，MBL）定律，可实时监测人体脑组织血氧含量的变化[6]，有助于医生对术中缺氧进行及时干预以及降低患者术后并发

症的发生概率。临床上主要以血氧饱和度作为脑氧含量的监测指标，血氧饱和度是组织中动脉、静脉、毛细血管氧饱和度的加权平均值，可反映氧供给与消耗的动态平衡状况[7]。使用 MBL 定律计算脑血氧饱和度时，差分路径因子（Differential Pathlength Factor，DPF）是用于计算脑血氧饱和度的重要变量之一，由于光子在人体皮肤组织中的传播具有前向散射特性，且在传播过程中不断发生吸收与散射，故光子的实际传播路径长度并不等同于光源与探测器的间距，需引入 DPF 对传播路径进行修正[8-9]。传统求解 DPF 的方法是通过多层生物组织蒙特卡罗模拟（Monte Carlo Modeling of Light Transport in Multi-Layered Tissues，MCML）对光子在生物组织内的传播轨迹进行仿真[10-11]，再根据每个光子的仿真信息求解 DPF，步骤如下：首先设置光子的数

量、能量权重以及不同波长下各层脑组织的光学参数与厚度等并作为输入参数，其次在计算机中模拟每个光子的运动轨迹，记录每个光子在生物组织内的传播信息，最后提取光子传播距离以及出射位置等信息以计算 DPF。此过程计算量较大，模拟的光子数量至少为百万量级，导致与 DPF 相关的光子传播信息的提取较困难，计算每一个 DPF 均需要耗费大量时间，无法实现批量运算，故现有的近红外脑血氧监测仪器算法通常将 DPF 设置为常量[12]。然而，DPF 与各层脑组织的光学参数与厚度等因素有关，不同个体脑组织的光学参数与厚度的差异较大，导致 DPF 的个体差异性较大，若设为常数，实际测量中将无法精准反映不同个体的脑血氧参数变化。

因此，本文采用支持向量机（Support Vector Machine，SVM）并结合网格寻优（Grid Search，GS），提出了一种基于 GS-SVM 的脑组织差分路径因子定量方法。首先选取不同年龄段人群的各层脑组织光学参数与厚度作为实验的输入数据，并对样本输入数据进行归一化以及主成分分析等预处理操作，其次建立了基于 GS-SVM 的脑组织差分路径因子预测模型对 DPF 进行快速预测，最后将实验结果与反向传播人工神经网络（Back Propagation Artificial Neural Network，BP-ANN）的预测结果进行比对。所提方法可有效解决蒙特卡罗模拟计算 DPF 时耗时长、提取参数复杂等缺点，有望对脑组织 DPF 实现准确、批量的计算。

2　实验部分

2.1　样本建立

人脑组成成分复杂，分别由头皮颅骨、脑脊液、灰质和白质组成[13]。利用近红外光谱检测脑血氧参数的方法是将相隔一段距离的光源与多个光电探测器放置于人体额头两端，根据近远端光电探测器接收到的光强变化，反演计算脑血氧生理参数。由于脑组织对光子的强散射性，光子在人脑内的传播路径近似于圆弧状[14]，蒙特卡罗模拟是在计算机中模拟光子在组织内的传播与出射过程，根据每个光子的传播信息求解 DPF 数值。蒙特卡罗模拟计算 DPF 的主要输入变量为各层脑组织的厚度、散射系数、吸收系数、各向异性因子以及折射率，表 1 所示为 800 nm 波长下某成人各层脑组织的厚度与光学参数。不同年龄段人群的脑组织厚度差异较大[15]，根据不同年龄段人群的脑组织厚度范围以及不同波长下血红蛋白的吸收与散射系数[16-19]，选取 120 组 0～50 岁年龄段人群每层脑组织的厚度与光学参数作为实验样本的初始变量，代入 MCML 程序中模拟计算 120 组 DPF 数值。首先根据仿真结果提取每个光子的传播路径与能量权重，再计算得到平均光学路径长度：

$$s = \frac{\sum\limits_i (s_i \cdot W_i)}{\sum\limits_i W_i}, \tag{1}$$

式中：s 是光子的平均光学路径长度；s_i 为蒙特卡罗模拟中第 i 个光子的传播路径长度；W_i 为第 i 个光子的能量权重。最后根据平均光学路径长度计算求解 DPF 数值：

$$s = D_P \times r, \tag{2}$$

式中：D_P 为 DPF；r 为光源与光电探测器间的距离。将蒙特卡罗模拟计算得到的 120 组 DPF 值作为实验样本的输出值。实验输入值与蒙特卡罗模拟输入参数一致，随机选取其中 90 组样本作为训练集，30 组样本作为测试集。训练集的输入参数为 90 行 20 列的矩阵，每行为不同参数下蒙特卡罗模拟计算 DPF 数值的一个样本，每列分别对应着每层脑组织的厚度、散射系数、吸收系数、各向异性因子以及折射率。测试集与训练集的输入参数类型相同，样本量为 30 个。

表 1　800 nm 波长下某成人脑组织的厚度与光学参数

Table 1　Thickness and optical parameters of certain adult brain tissue at 800 nm wavelength

Brain tissue	Thickness d /cm	Scattering coefficient μ_s/cm^{-1}	Absorption coefficient μ_a/cm^{-1}	Anisotropy factor g	Refractive index n
Scalp and skull	1	17.5	0.17	0.90	1.4
Cerebrospinal fluid	0.2	0.1	0.01	0.92	1.4
Gray matter	0.4	22	0.36	0.89	1.4
White matter	20	91	0.14	0.90	1.4

2.2 数据预处理

在实验输入数据中,各层脑组织的光学参数差异较大,且每层脑组织的各向异性因子以及折射率较为接近,为了提高实验精度以及防止回归模拟器过拟合,采用均值归一化与主成分分析(Principal Component Analysis,PCA)法对实验输入数据进行预处理[20-21]。首先对所有输入数据进行均值归一化处理,使输入数据范围固定在 0~1 之间。归一化处理的目的是保证样本各特征变量对实验结果的贡献率一致,使样本各特征变量保持在同一数量级,减少样本各特征变量相差过大对实验结果的影响。接着采用 PCA 法对归一化后的数据进行降维处理。实验中单个样本的总维度为 20,依次为每层脑组织的厚度、散射系数、吸收系数、各向异性因子以及折射率,经过 PCA 处理后,样本数据映射为 5 维无物理意义的数学变量。每一维数据的主成分占比如表 2 所示,可以看出,降维后各成分的累计贡献率达到 96.4%,故可使用 PCA 降维后的数据代替原本 20 维的输入数据作为实验输入,精简回归模拟器模型输入参数,降低噪声干扰。

表 2 降维后的主成分占比

Table 2 Proportion of principal component after dimensionality reduction

Component	Proportion of principal component
PC1	67.7
PC2	10.7
PC3	7.9
PC4	5.1
PC5	5.0

2.3 构建 GS-SVM 预测模型

支持向量机是一种支持小样本容量的机器学习算法,可以快速地将原始样本通过径向核函数映射至高维线性特征空间中,有效地对数据进行分类与回归处理[22-23]。网格寻优算法通过遍历网格,找到合适的惩罚参数(C)与高斯核函数的参数(g),使得回归模拟器的均方误差(MSE)达到最小[24]。上述两种算法的结合可准确有效地对实验数据进行回归处理。设置初始参数,采用 Matlab 构建基于 GS-SVM 的脑组织差分路径因子预测模型:首先设置步长并划分网格,其次通过不断遍历网格中的值,搜寻最佳的 C 与 g,最后通过交叉验证(Cross Validation,CV)来验证每组回归模拟器的性能[25-26],将回归模

拟器的均方误差作为该参数下模型优劣的评判标准。具体流程如图 1 所示,其中 C 的范围设为 $[2^{-8}, 2^8]$,g 的范围设为 $[2^{-8}, 2^8]$,C 与 g 的步长均定为 0.5,交叉验证参数 k 取 3。
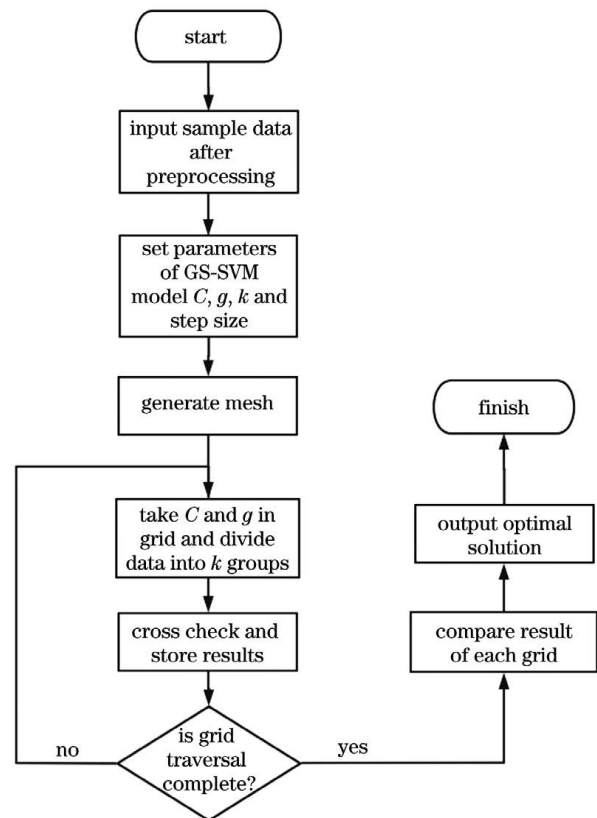

图 1 基于 GS-SVM 的脑组织差分路径因子预测模型流程图

Fig. 1 Flow chart of brain tissue differential pathlength factor prediction model based on GS-SVM

3 结果与讨论

将经过归一化与 PCA 处理后的数据代入到基于 GS-SVM 的脑组织差分路径因子预测模型中进行实验。网格寻优算法的计算结果如图 2 所示。可以看出,当惩罚参数 C 为 5.278,高斯核函数的参数
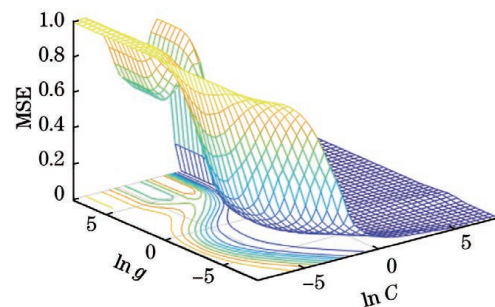

图 2 网格寻优后的 SVM 参数选择图

Fig. 2 SVM parameter selection diagram after grid optimization

g 为 0.082 时,该回归模拟器的均方误差最小,为 0.0013796。

使用上述最优参数的预测模型对测试集数据进行回归预测。相较于测试集的输出数据,基于 GS-SVM 的脑组织差分路径因子预测模型的均方误差为 0.0268,在 Win10 系统 CPU 型号为 i5-9500 的操作平台下,程序运行时间为 1.52 s,测试集输出数据为蒙特卡罗模拟预测的 DPF 数值。在同一操作平台下,使用蒙特卡罗模拟计算单个 DPF 的时间大约为 4 min,不同参数下的计算时间不同,计算 120 组数据总耗时约 8 h,共计 28943 s,而基于 GS-SVM 模型计算 120 组 DPF 仅仅需要 1.52 s,运算速度有明显提高。采用 BP-ANN 预测模型进行对比实验,隐含层的层数设置为两层,使用与 GS-SVM 预测模型相同的训练集与测试集。相较于蒙特卡罗模拟,BP-ANN 预测结果的 MSE 为 0.25,以上两种预测模型与蒙特卡罗模拟预测结果的对比如图 3 所示。图 4 所示为两种预测模型与蒙特卡罗模拟预测结果的相关性分析图。由图 4 可得,GS-SVM 与 BP-ANN 预测模型均与蒙特卡罗模拟预测结果呈显著性相关(显著水平 $P < 0.0001$),相关系数(R^2)分别为 0.97 与 0.92。BP-ANN 与 GS-SVM 预测模型的实验对比结果如表 3 所示,相比之下,GS-SVM 预测模型的预测结果优于 BP-ANN 预测模型,且与模特卡罗模拟预测结果更为接近。
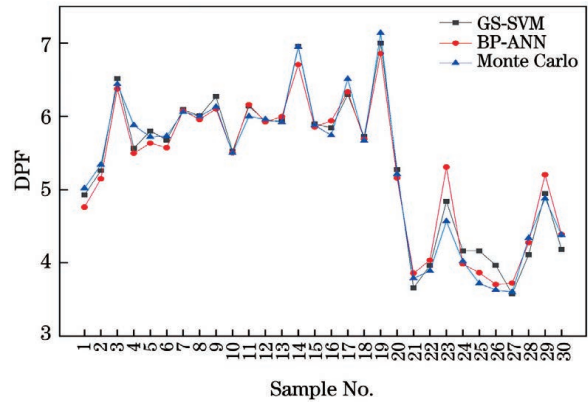

图 3　GS-SVM 和 BP-ANN 预测模型与蒙特卡罗模拟的预测结果对比

Fig. 3　Comparison of prediction results given by Monte Carlo simulation, GS-SVM and BP-ANN prediction models
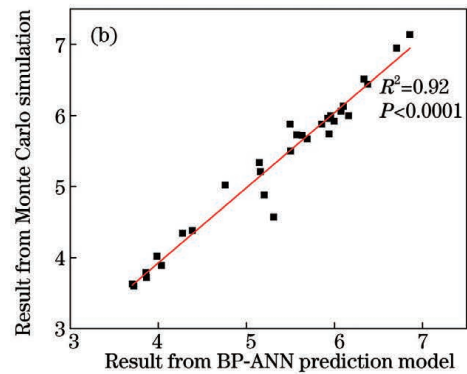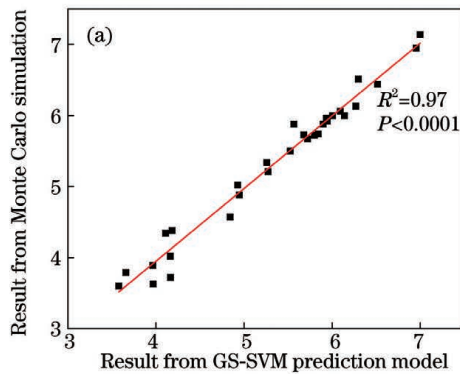

图 4　两种预测模型与蒙特卡罗模拟预测结果的相关性分析。(a)GS-SVM 预测模型;(b)BP-ANN 预测模型

Fig. 4　Correlation analysis of prediction results given by two prediction models and Monte Carlo simulation. (a) GS-SVM prediction model; (b) BP-ANN prediction model

表 3　BP-ANN 与 GS-SVM 预测模型的实验结果对比

Table 3　Comparison of experimental results between BP-ANN and GS-SVM prediction models

Prediction model	MSE	R^2
GS-SVM	0.0268	0.97
BP-ANN	0.25	0.92

4　结　　论

建立了基于 GS-SVM 的脑组织差分路径因子预测模型,对脑组织 DPF 值进行了快速预测,并将此方法与 BP-ANN 预测模型进行了对比。结果表明,网格寻优算法可以自动、准确地对惩罚参数 C 与高斯核函数的参数 g 进行寻优,基于 GS-SVM 的脑组织差分路径因子预测模型的预测结果优于 BP-ANN,与蒙特卡罗模拟方法的预测结果呈显著的相关性,有望代替蒙特卡罗模拟方法对 DPF 数值进行批量计算。所提方法可应用于近红外脑血氧监测仪器中,使得脑血氧代谢生理参数的计算更加快速、准确。

参 考 文 献

[1]　Chan M J, Chung T, Glassford N J, et al. Near-infrared spectroscopy in adult cardiac surgery

patients: a systematic review and meta-analysis[J]. Journal of Cardiothoracic and Vascular Anesthesia, 2017, 31(4): 1155-1165.

[2] Aguirre J A, Etzensperger F, Brada M, et al. The beach chair position for shoulder surgery in intravenous general anesthesia and controlled hypotension: impact on cerebral oxygenation, cerebral blood flow and neurobehavioral outcome[J]. Journal of Clinical Anesthesia, 2019, 53: 40-48.

[3] Yu Y, Lyu Y, Jin L, et al. Prognostic factors for permanent neurological dysfunction after total aortic arch replacement with regional cerebral oxygen saturation monitoring[J]. Brain and Behavior, 2019, 9(7): e01309.

[4] Bale G, Elwell C E, Tachtsidis I. From Jöbsis to the present day: a review of clinical near-infrared spectroscopy measurements of cerebral cytochrome-c-oxidase[J]. Journal of Biomedical Optics, 2016, 21 (9): 091307.

[5] Ferrari M, Mottola L, Quaresima V. Principles, techniques, and limitations of near infrared spectroscopy [J]. Canadian Journal of Applied Physiology, 2004, 29(4): 463-487.

[6] Delpy D T, Cope M, van der Zee P, et al. Estimation of optical pathlength through tissue from direct time of flight measurement[J]. Physics in Medicine and Biology, 1988, 33(12): 1433-1442.

[7] Rolon R E, Gareis I E, Larrateguy L D, et al. Automatic scoring of apnea and hypopnea events using blood oxygen saturation signals[J]. Biomedical Signal Processing and Control, 2020, 62: 102062.

[8] Chiarelli A M, Perpetuini D, Filippini C, et al. Differential pathlength factor in continuous wave functional near-infrared spectroscopy: reducing hemoglobin's cross talk in high-density recordings [J]. Neurophotonics, 2019, 6(3): 035005.

[9] Chatterjee S, Abay T Y, Phillips J P, et al. Investigating optical path and differential pathlength factor in reflectance photoplethysmography for the assessment of perfusion[J]. Journal of Biomedical Optics, 2018, 23(7): 075005.

[10] Wang L H, Jacques S L, Zheng L Q. MCML: Monte Carlo modeling of light transport in multi-layered tissues[J]. Computer Methods and Programs in Biomedicine, 1995, 47(2): 131-146.

[11] Ding H S, Wang F, Su C, et al. Simulation and application for near infrared light transport in biological tissues[J]. Journal of Tsinghua University (Science and Technology), 1999, 39(9): 5-8.
丁海曙, 王峰, 苏畅, 等. 近红外光子在生物组织中迁移的仿真及应用[J]. 清华大学学报(自然科学版), 1999, 39(9): 5-8.

[12] Feng W, Haishu D, Fenghua T, et al. Influence of overlying tissue and probe geometry on the sensitivity of a near-infrared tissue oximeter[J]. Physiological Measurement, 2001, 22(1): 201-208.

[13] Kümmel T, van Marwick B, Rittel M, et al. Rapid brain structure and tumour margin detection on whole frozen tissue sections by fast multiphotometric mid-infrared scanning[J]. Scientific Reports, 2021, 11 (1): 11307.

[14] Fantini S, Franceschini M A, Maier J S, et al. Frequency-domain multichannel optical detector for noninvasive tissue spectroscopy and oximetry[J]. Optical Engineering, 1995, 34(1): 32-42.

[15] Almuhawas F A, Dhanasingh A E, Mitrovic D, et al. Age as a factor of growth in mastoid thickness and skull width[J]. Otology & Neurotology, 2020, 41(5): 709-714.

[16] Scholkmann F, Wolf M. General equation for the differential pathlength factor of the frontal human head depending on wavelength and age[J]. Journal of Biomedical Optics, 2013, 18(10): 105004.

[17] Bashkatov A N, Genina E A, Tuchin V V. Optical properties of skin, subcutaneous, and muscle tissues: a review[J]. Journal of Innovative Optical Health Sciences, 2011, 4(1): 9-38.

[18] Marois M, Jacques S L, Paulsen K D. Optimal wavelength selection for optical spectroscopy of hemoglobin and water within a simulated light-scattering tissue[J]. Journal of Biomedical Optics, 2018, 23(7): 071202.

[19] Matcher S J, Elwell C E, Cooper C E, et al. Performance comparison of several published tissue near-infrared spectroscopy algorithms[J]. Analytical Biochemistry, 1995, 227(1): 54-68.

[20] Lei X D, Wang H T, Zhao Z Z. Small-sample airborne LiDAR point cloud classification based on transfer learning and fully convolutional network[J]. Chinese Journal of Lasers, 2021, 48(16): 1610001.
雷相达, 王宏涛, 赵宗泽. 整合迁移学习与全卷积网络的小样本机载激光雷达点云分类[J]. 中国激光, 2021, 48(16): 1610001.

[21] Wang Q, Zeng W D, Xia Z P, et al. Recognition of food-borne pathogenic bacteria by Raman spectroscopy based on random forest algorithm[J]. Chinese Journal of Lasers, 2021, 48(3): 0311002.
王其, 曾万聃, 夏志平, 等. 基于随机森林算法的食源性致病菌拉曼光谱识别[J]. 中国激光, 2021, 48 (3): 0311002.

[22] Pasadas D J, Ramos H G, Feng B, et al. Defect classification with SVM and wideband excitation in

multilayer aluminum plates[J]. IEEE Transactions on Instrumentation and Measurement, 2020, 69(1): 241-248.

[23] Wang S T, Zhan S J, Liu S Y, et al. Classification and identification of sex hormones by three-dimensional fluorescence spectroscopy combined with ICSO-SVM[J]. Acta Optica Sinica, 2021, 41(10): 1030004.
王书涛, 展书杰, 刘诗瑜, 等. 三维荧光光谱结合 ICSO-SVM 对性激素的分类鉴别[J]. 光学学报, 2021, 41(10): 1030004.

[24] Fayed H A, Atiya A F. Speed up grid-search for parameter selection of support vector machines[J]. Applied Soft Computing, 2019, 80: 202-210.

[25] Qiu S L, Li A, Wang X S, et al. High-accuracy quantitatively analysis of iron content in mineral based on laser-induced breakdown spectroscopy[J]. Chinese Journal of Lasers, 2021, 48(16): 1611002.
邱苏玲, 李安, 王宪双, 等. 基于激光诱导击穿光谱的矿石中铁含量的高准确度定量分析[J]. 中国激光, 2021, 48(16): 1611002.

[26] Lu X Y, Yun T, Xue L F, et al. Effective feature extraction and identification method based on tree laser point cloud[J]. Chinese Journal of Lasers, 2019, 46(5): 0510002.
卢晓艺, 云挺, 薛联凤, 等. 基于树木激光点云的有效特征抽取与识别方法[J]. 中国激光, 2019, 46(5): 0510002.

Quantitative Methods of Brain Tissue Differential Pathlength Factor Based on GS-SVM

Chu Bao[1,2], Huang Yao[2,3*], Ni Jingshu[2,3], Zhang Chijian[1], Li Zhongsheng[2,3], Zhang Yuanzhi[2,3], Dong Meili[2,3], Wang Quanfu[2,3], Wang Xia[2,3], Wang Yikun[2,3**]

[1] *College of Physics and Electronic Information, Anhui Normal University, Wuhu, Anhui 241000, China;*

[2] *Anhui Provincial Engineering Laboratory for Medical Optical Diagnosis & Treatment Technology and Instrument, Anhui Institute of Optics and Fine Mechanics, Hefei Institute of Physical Science, Chinese Academy of Science, Hefei, Anhui 230026, China;*

[3] *Anhui Provincial Engineering Technology Research Center for Biomedical Optical Instrument, Wanjiang Center for Development of Emerging Industrial Technology, Tongling, Anhui 244000, China*

Abstract

Objective Brain blood oxygen monitoring based on near infrared spectroscopy can display the state of oxygen supply and demand in the brain noninvasively, continuously and in real time. It is very important for brain protection in surgery and has high application value in many departments of the hospital. Differential pathlength factor (DPF) is one of the important variables for calculating cerebral oxygen saturation. Because photons propagate in human skin tissues with forward scattering characteristics and absorption and scattering occur continuously in the propagation process, the actual propagation path length of photons is not equal to the distance between the light source and the detector, so a DPF should be introduced to correct the propagation path length. The traditional method to obtain the DPF is to first simulate the propagation trajectories of photons in biological tissues through Monte Carlo modeling of light transport in multi-layered tissues, and then give the DPF according to the simulation information of each photon. The amount of calculation in this process is large and the simulated order of magnitude of photon is at least one million, which make it difficult to extract the photon propagation information related to the DPF. It takes a lot of time to calculate each DPF, and batch operation cannot be realized. Therefore, a DPF is usually set as a constant in the existing algorithms of near-infrared cerebral oxygen monitoring instrument. However, a DPF is related to the optical parameters and thickness of each layer of one brain tissue. There are great differences in the optical parameters and thicknesses of different individual brain tissues, resulting in great individual differences in the DPF. If it is set as a constant, the actual measurement will not accurately reflect the changes of cerebral blood oxygen parameters of different individuals.

Methods In view of the above shortcomings, a fast DPF quantitative calculation method is proposed in this paper. First, 120 groups of people aged at 0–50 years are selected as the initial variables of the experimental samples, and 120 groups of DPF values are simulated and calculated in the MCML program as the initial experimental variables, of

which 90 groups are used as the training dataset and 30 groups are used as the test dataset. Because the optical parameters of each layer of the brain tissue for the experimental input data vary greatly and the anisotropy factor and the refractive index of each layer of the brain tissue are close, in order to improve the experimental accuracy and prevent overfitting of the regression simulator, the mean normalization and the principal component analysis are used to preprocess the experimental input data. Second, support vector machine (SVM) combined with grid search (GS) is used to establish the prediction model of brain tissue differential pathlength factor based on GS-SVM. Support vector machine can quickly map the original samples to a high-dimensional linear feature space through a radial kernel function, and effectively classify and regress the data. The grid optimization algorithm finds the appropriate penalty parameter C and the parameter g of the Gaussian kernel function by traversing the grid, so as to minimize the mean square error of the regression simulator. Finally, the prediction model is used to back judge the test dataset and its results are compared with the prediction results of the back propagation artificial neural network (BP-ANN). The number of hidden layers is set to two, and the same training set and test set in the GS-SVM prediction model are used.

Results and Discussions　　The results show that, compared with the results of Monte Carlo simulation, the mean square errors (MSE) of the GS-SVM prediction model and the BP-ANN prediction model are 0.0268 and 0.25, and the correlation coefficients (R^2) are 0.97 and 0.92, respectively (Fig. 3). The prediction result of the brain tissue differential pathlength factor quantitative model based on GS-SVM is better than that based on BP-ANN (Table 3), which is significantly correlated with the result of the Monte Carlo simulation (Fig. 4). In the Win10 system under the operating platform with i5-9500 CPU and 8 GB memory, it takes about 4 min to calculate a single DPF using Monte Carlo simulation. The calculation time under different parameters is different. The total time for calculating 120 groups of data is about 8 h, totaling 28943 s, in contrast, it takes only 1.52 s to calculate 120 groups of DPF based on the GS-SVM model and the calculation speed is significantly improved.

Conclusions　　In this paper, a brain tissue differential pathlength factor prediction model based on GS-SVM is established to quickly predict the DPF value of a brain tissue, and this method is compared with the BP-ANN prediction model. The results show that the grid optimization algorithm can automatically and accurately optimize the penalty parameter C and the parameter g of the Gaussian kernel function. The prediction results of the brain tissue differential pathlength factor prediction model based on GS-SVM are better than those based on BP-ANN, and have significant correlation with the prediction results of the Monte Carlo simulation method. It is expected to replace the Monte Carlo simulation method for batch calculation of DPF values. It can be applied in the near infrared cerebral oxygen monitoring instrument to make the calculation of physiological parameters of cerebral oxygen metabolism more rapid and accurate.

Key words　　medical optics; near infrared spectroscopy; differential pathlength factor; Monte Carlo simulation; support vector machine; grid search